Analytical and numerical estimation of the q-behaviour factor of structural glass frames

Chiara Bedon [a], Manuel Santarsiero [b]

[a] *Department of Engineering and Architecture, University of Trieste, Piazzale Europa 1, 34127 Trieste, Italy*

[b] *Federal Office of Roads and Infrastructures, FEDRO, Switzerland*

Keywords: Seismic design; glass frames; analytical method; Finite Element (FE) numerical modelling; q-behaviour factor

ABSTRACT

In the Italian and international scenario, current design standards for seismic resistant buildings provide recommendations for the advanced analysis of several structures subjected to earthquakes, but no specific details are given for structural glass systems. There, critical design issues for glazed structures may derive from the lack of appropriate resistance but also from the limited accommodation of displacement demands. Consequently, joints and restraints can have a key role for design optimization purposes. This paper presents an energy-based analytical study and a refined Finite Element (FE) numerical analysis for a case-study glass frame, showing the potentials, limits and issues of the calculations approaches, towards the definition of preliminary design estimates for earthquake resistant glass frames. Special care is spent for the potential ductile and dissipative behaviour of structural glass frames, with some recommendations for the *q*-behaviour factor.

1 INTRODUCTION

From a structural point of view, ordinary assemblies composed of conventional constructional materials and located in seismic regions are commonly required to offer adequate safety and serviceability performance capacities, namely represented by:

- a limited probability of collapse (even in presence of yielding and extensive structural damages); and
- an appropriate capacity to accommodate the displacement demands.

Figure 1. Example of an existing seismic-resistant glass pavilion (reproduced from (Santarsiero et al. 2019)).

Structural glass, in this regard, represents an innovative material that should satisfy specific resistance and displacement demands, even under extreme design loads. This can be the case of curtain walls, simple load-bearing members (i.e., beams, columns), or complex 3D systems and stand-alone structures (see for example Figure 1). Dedicated design methods and a special care for details is thus required (Bedon et al., 2018).

However, the challenge for glass designers is even more complex, because no detailed attention is given by standards to assess (or improve) the seismic performance of glass systems (see for example (EN 1998-1:2004, NTC2018), etc.). As a general rule, most of the seismic requirements of current standards are in fact related to general considerations for "*non-structural*" components, hence focused on providing adequate gaps to accommodate the relative displacements of primary buildings, etc.

At the same time, limited research investigations have been focused on the seismic performance and design of glass structures, and the available studies are mostly related to specific constructional typologies. For example, research efforts have been spent in (Sucuoglu and

Vallabhan, 1997; Wensheng and Baofeng, 2008; Sivanerupan et al. 2011) for curtain walls with glass components fully braced by continuous metal frames. Their dissipation capacity under seismic events was experimentally explored by (Casagrande et al. 2019). Bedon and Amadio (2018) proved that ordinary curtain walls can be efficiently involved in the dynamic response of multi-storey buildings under seismic events, based on special connectors allowing to realize a "distributed-TMD" concept. Few studies can be then found for point-supported facades, and their drift performance under in-plane lateral loads, see (Martins and Delgado, 2012; Sivanerupan et al. 2014; etc.). In (Krstevska et al. 2013) the dissipation capacity of novel, composite timber-glass walls able to actively contribute to the seismic performance of primary buildings was assessed. In this paper, the seismic behaviour of glass frames is investigated, with special consideration for the preliminary estimate of their expected *q*-behaviour factor.

2 SEISMIC DESIGN OF GLASS STRUCTURES IN ITALY

2.1 Basis of design

Section §4.4 of CNR-DT 210/2013 focuses on seismic design actions and general rules for safe design purposes. The CNR guide includes a pre-standard study on the performance of glass structures and is not prescriptive. However, it actually represents one of the most detailed guides in support of glass designers, given the lack of specific regulations in the Italian Technical Standards for Constructions (NTC2018). In addition, several sections are supporting the drafting of the in-progress Eurocode 10 for glass structures, see also (Feldmann et al. 2014).

2.2 Consequences classes

For seismic purposes, the CNR document detects different levels of analysis and design for structural glass systems / elements. These are implicitly related to their class of use and consequences classes (CC). A given glass system / element is in fact expected to belong to classes CC1 to CC3. Otherwise, the guide disregards all the glass elements that do not have any kind of structural role, and fall in the CC0 (see also §3.2.1 and EN1990:2002-Annex B1). More in detail:

- CC1= when glass failure has *limited* consequences in terms of loss of human life and *small or negligible* consequences in economic, social or environmental terms. CC1 includes glass structures / elements in buildings with people present only occasionally;
- CC2= when failure has *medium* consequences for human life, but *considerable* consequences in economic, social and environmental terms. Typical examples are glass structures / elements for residential / office buildings;
- CC3= when failure has *high* consequences in terms of human life and *very great* consequences in economic, social terms. CC3 includes public buildings and places susceptible to overcrowding.

Some typical examples of CC are reported in Table 1. There – compared to other constructional materials – it is possible to see that the appropriate verification of glass structures can be implicitly related to uncertainties, when designers are asked to associate a given element / system to a certain CC. Special care is hence required for such a delicate aspect, in favour of appropriate and safe verifications.

Table 1. Classification of common glass elements (CC0= secondary, non-structural elements). n.a.= no performance assessment is required; F= failure

Element	CC_n (pre-F)	CC_n (post-F)
Vertical (linear restraints)	1	1/n.a.
Vertical (point fixings)	2/1	1/n.a.
Roofs	2	2/1
Fins	2	2/1
Railings (fall danger)	2	2/1
Floors, beams	2	2
Pillars	3	2 (pre-F loads)

At the same time, it is important to recall that a key role is assigned not only to glass but also to the detailing of connectors.

For seismic design, the distinction of the CNR guide is thus between (a) "*secondary*" structural elements or (b) glass elements that have a relevant structural role under seismic events (§4.4.1).

The definition (a) is reliable as far as the stiffness and resistance of glass members can be neglected (that is, less than 15% the full system – see also NTC2018, §7.2.3). In other words, these elements can be disregarded in the global seismic analysis, but are in any case required to withstand vertical loads and accommodate the global deformations, under the most unfavourable seismic combination of loads. Both in-plane and out-of-plane seismic performances of glass components and joints must be properly verified, to preserve their load-bearing capacity. In case (b), the CNR guide includes all the glass systems / elements that have a relevant stiffness / resistance contribution, or consist of stand-alone / special glass structures. All these solutions fall in CC3, and even minor damage must be strictly avoided. Dedicated experimental tests are also recommended, in support of design.

2.3 Nominal design life and reference life

The seismic design action for glass systems / elements is then related to a series of key parameters, as in the case of constructions in general. The nominal life V_N, as usual, defines the period over which it is assumed that it can be safely used for the intended purposes (with scheduled maintenance). Commonly, it is assumed that also for glass structures V_N= 50 years, but other conditions may occur (Table 2).

Table 2. Definition of design life V_N (pre-failure [1]) for glass structures / elements

V_N (years)	Examples
10	Temporary structures [2]
10-25	Replaceable parts
15-30	Agricultural structures
50	Buildings, common structures
100	Monumental buildings, bridges, other

[1] Post-failure V_N= 10 years for CC1 and CC2; to derive from specific studies for CC3
[2] Excluded structures / parts that can be dismantled / reused

Certainly, see Table 2, a special care is spent for the distinction of V_N intervals in the range from 10 to 30 years, for "*temporary*" and "*replaceable*" structures that could involve the use of glass.

With reference to the consequences of interruption of service or ultimate failure, structural glass systems must then satisfy specific demands that are related to the *importance class* they belong, with:

- Class I= for occasional presence of people or agricultural buildings
- Class II= normal crowd levels or factories, without essential public / social functions
- Class III= significant crowd levels, and
- Class IV= important public or construction with strategic functions

Table 3. C_U factor as a function of the importance class

	Importance class			
	I	II	III	IV
C_U	0.7	1.0	1.5	2.0

The design seismic action hence depends on the reference life V_R, given by V_N and the class of use (C_U, see Table 3), that is:

$$V_R = V_N \times C_U \tag{1}$$

All the other relevant parameters for the definition of the seismic action – including the return-period T_R – can be found in §4.4.2.

2.4 Performance levels

In general, all the design recommendations of the CNR guide are aimed at improving the capacity of glass systems to accommodate the earthquakes demands. The primary goal is to limit possible risk for people, due to partial damage, shards or failure of glass elements. According to the conventional definition of Limit States (i.e., Operational (OLS), Damage (DLS), Safeguard of human life (SLS) and Collapse prevention (CLS)), the expected performances for glass systems are reported in Tables 4 and 5.

Table 4. Required performances for structural glass systems under seismic loads (see also Table 5). Subscript= T_R

	Importance class			
Limit State	I	II	III	IV
OLS	-	-	ND_{45}	ND_{60}
DLS	SD_{35}	SD_{50}	SD_{75}	SD_{100}
SLS	HD_{333}	HD_{475}	HD_{713}	HD_{950}
CLS	-	-	F_{1463}	F_{1950}

Table 5. Definition of performance levels

Performance level		Description
ND	No damage	No damage in glass; no replacement; watertightness preserved
SD	Slight damage	Partial loss of functionality; usable building; no risk for users
HD	Heavy damage	High degree (and cost) of functionality loss; still no risk for users
F	Failure	Severe damage; evidence of failure; risk for users

2.5 Design seismic force and q-behaviour factor

When more detailed methods of analysis are not available, the global and local seismic verification of a given glass assembly can be carried out by taking into account an horizontal force given by (§4.4.3):

$$F_a = \frac{S_a W_a}{q} \tag{2}$$

where:

W_a	is the weight of the element,
q	the behaviour factor,
S_a	the peak acceleration.

As far as an individual glass element is verified against out-of-plane seismic loads, an equivalent seismic pressure can be used, based on Eq.(2). In that case, the peak acceleration is given by:

$$S_a = \frac{a_g}{g} \cdot S \cdot R_a \qquad (3)$$

with the magnification factor equal to:

$$R_a = max\begin{cases} \frac{3(1+Z/H)}{1+(1-T_a/T_1)^2} - 0.5 \\ 1 \end{cases} \qquad (4)$$

and:

- a_g the peak ground acceleration (rock soil) for the LS of interest;
- g the acceleration of gravity;
- S accounts for soil category and topographical conditions;
- Z the height of centre of gravity of the glass element (from the foundation);
- H the height of the assembly / building (from the foundation);
- T_a the fundamental period of glass;
- T_1 the fundamental period of the full assembly / building, in the direction of interest.

Actually, however, the behaviour factor q of Eq.(2) represents one of the critical aspects for the design of glass structures in seismic regions.

No specific recommendations are in fact available, and such a lack turns out in analyses and verifications that are generally carried out with q= 1. On one side, wide safety levels can be preserved for a given glass structure. On the other hand, the system itself could be overdesigned, even in presence of joints with relevant ductility and dissipation capacity. In this paper, some seismic design considerations are proposed for glass portal frames, giving evidence of their current potentials and criticalities under extreme loads.

3 CASE-STUDY EXAMPLE

3.1 Description of the system and seismic analysis

Following section 2, the case-study system agrees with Figure 2(a) and can be intended as a stand-alone structural system composed of laminated glass (LG), with relevant risk for people in case of damage.

More in detail, the frame consists of two H= 6m high columns and a beam with L= 8m of span, and all the LG structural members are made of heat-strengthened glass, with uniform cross-section (h= 600mm high × t_{tot}= 66mm thick), obtained via 5× t_g= 12mm glass layers bonded by t_{int}= 1.52mm thick ionoplast interlayer foils (SG type).

Each beam-to-column mechanical connection is realized in the form of an ideal pin, so as to allow a more efficient accommodation of the vertical deformations of the structure (i.e., due to live loads, creep phenomena, etc.).

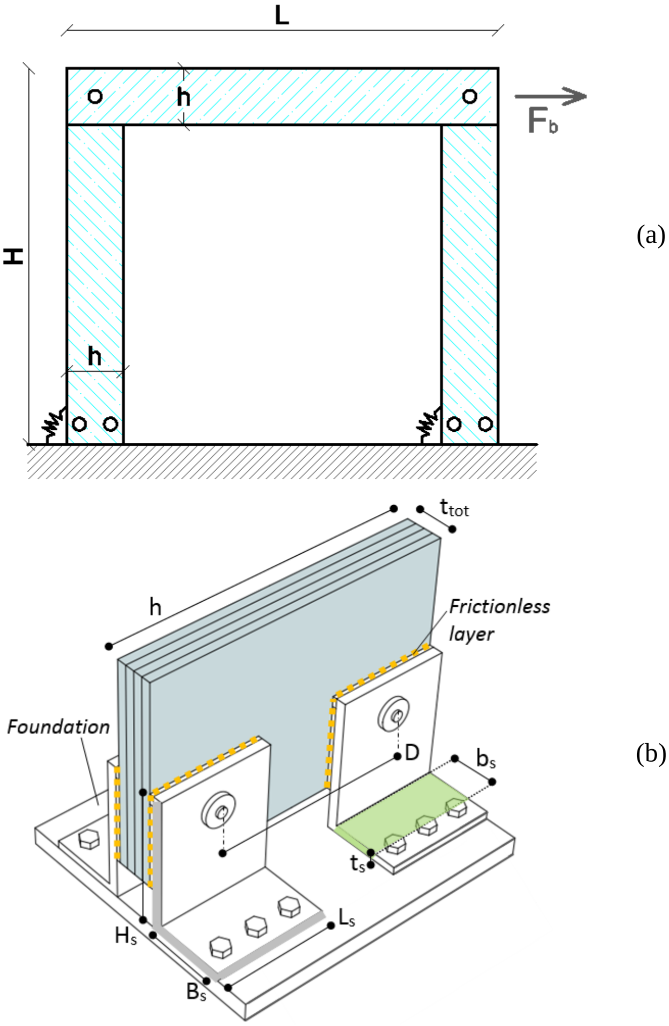

Figure 2. Case-study glass frame: (a) lateral view and (b) detail of the base connection.

In addition, the lateral stability of the frame under in-plane seismic loads is achieved through push-pull moment connections at the base of the columns (see Figure 2(b)). Possible out-of-plane deformations of the frame, finally, are assumed to be restrained by bracing members (disregarded in the current research study) belonging to the full 3D glazed assembly (i.e., modular units).

The base restraints of Figure 2(b), in particular, include two stainless steel pins (ϕ= 24mm the nominal diameter, D= 500mm the distance), passing through ϕ_g= 32mm holes in the LG section. Four mild steel brackets composed of S235 steel are used to restrain each column to the foundation (t_s= 15mm the thickness, with B_s=

200mm (b_s= 165mm) × H_s= 300mm × L_s= 200mm). The brackets are then fixed to the base foundation via n_b anchoring bolts. While providing a mostly rigid restraint of the frame towards ordinary design loads, the so-assembled connections have a key role especially in seismic conditions. The resisting mechanism of each device, in particular, is mostly related to the bending response of the $b_s \times t_s$ plate, with $b_s < B_s$.

For seismic calculations, the glass frame is assumed located in a high seismicity region of Italy (S_d= 0.35g the ground acceleration). Disregarding the vertical dead loads and according to Eq.(2), the in-plane lateral force the frame should resist is given by:

$$F_a \approx \frac{103\ kN}{q} \quad (5)$$

Such an in-plane shear load would correspond (for a single LG column in bending) to a stress concentration in the region of holes, as schematized in Figure 3.

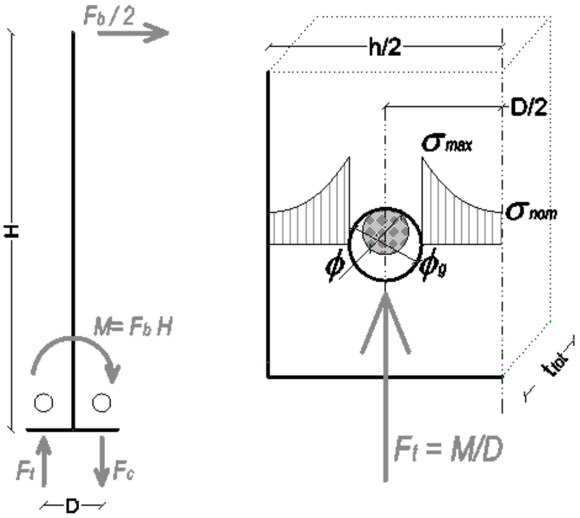

Figure 3. Stress peaks at the base of a glass column under seismic loads

Given the stress value:

$$\sigma_{nom} = \frac{F_t}{(\frac{h}{2} - \phi_g) \cdot t_{tot}} \quad (6)$$

the expected maximum peak is in fact equal to:

$$\sigma_{max} = K_t \cdot \sigma_{nom} \quad (7)$$

with K_t the magnification factor of stresses, depending on the hole diameter, the size of the plate and the type of load. Typical values for glass plates under in-plane loads in the range of K_t= 2-2.5 (see also (Mocibob, 2008)). Similar considerations can be then extended to the brackets in compression, thus representing a key parameter for design of the structural details of the frame.

4 ANALYTICAL MODEL

To estimate a reliable *q*-behaviour factor for the examined glass frame, simple analytical calculations could be taken into account (see also (Santarsiero et al., 2019). More in detail, it is assumed that the ductility of the full system is offered by the steel angle brackets of Figure 2(b). Given that in-plane elastic deformations of the glass beams / columns can be reasonably disregarded, the lateral drift of the frame Δ can be thus estimated as a function of the vertical displacement δ and rotation φ of the steel brackets in tension, with (see also Figure 4):

$$\Delta(\delta) = \frac{H}{D} \cdot \delta \quad (8)$$

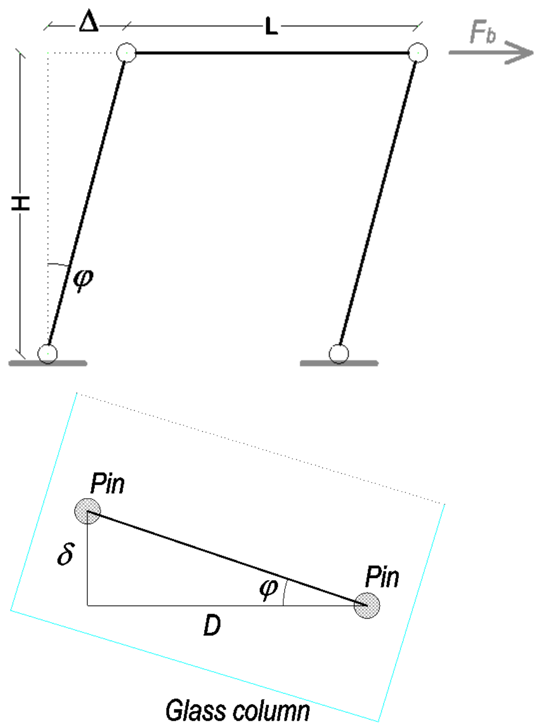

(a)

(b)

Figure 4. Mathematical model for glass frames under seismic loads. (a) Reference system and (b) detail of deformations in the base connection

The vertical deformation of the brackets at first yielding derives from the maximum moment M that the frame transfers to the foundation, and the connection can resist, that is:

$$\delta_y = \frac{f_y \cdot b_s^2}{3 E_s t_s} \quad (9a)$$

where δ_y is obtained by equalling:

$$M = \frac{6 \cdot E_s I \cdot \delta_y}{b_s^2} \quad (9b)$$

and:

$$M_y = W_y \cdot f_y = \frac{b_s t_s^2}{6} \cdot f_y \quad (9c)$$

Similarly, the vertical deformation of the brackets at failure depends on the occurrence of plastic mechanisms in the angles in tension, where a maximum extension can be expected up to:

$$L_{pl} = \frac{b_s}{2} - x = \frac{b_s}{2} \cdot (1 - \frac{M_y}{M_{pl}}) \tag{10}$$

Assuming that the rotation point is at the centre of the hinge, the deformation δ_u of the bracket at failure corresponds to:

$$\delta_u = \delta_y + \theta_{pl} \cdot (b_s - L_{pl}) \tag{11}$$

with δ_y given by Eq.(9a) and θ_{pl} the ultimate plastic curvature:

$$\theta_{pl} = L_{pl} \cdot \frac{\varepsilon_y}{t_s/2} + \frac{L_{pl} \cdot \left(\frac{\varepsilon_u}{t_s/2} - \frac{\varepsilon_y}{t_s/2}\right)}{2} = \frac{L_{pl} \cdot (\varepsilon_y + \varepsilon_u)}{t_s} \tag{12}$$

Following Eqs.(9a) and (11), the ductility that each steel bracket can offer is thus given by:

$$\mu = \frac{\delta_u}{\delta_y} \tag{13}$$

and hence:

$$q = \sqrt{2\mu - 1} \geq 1 \tag{14}$$

5 FINITE ELEMENT NUMERICAL MODELLING

5.1 Methods

In order to explore more in detail the in-plane seismic performance of the case-study system of Figure 2, as well as assess the validity of the analytical approach proposed in section 4, a refined FE model was described in ABAQUS (Simulia, 2019). The typical analysis consisted of a displacement-controlled static simulation, where a linear increasing in-plane lateral displacement U_x was assigned at the top of the column (H= 6m), and the structural effects induced at the base of the frame were analysed in detail.

In accordance with Figure 5, in particular, all the FE components were described in the form of full 3D brick elements (C3D8R type from ABAQUS library), so as to reproduce the local and global behaviour of the involved mechanical components. The key geometrical and mechanical input assumptions for glass and steel members (including contact interactions) were derived from past research efforts, see also (Santarsiero et al. 2018; Bedon & Louter, 2019; Santarsiero et al. 2019).

A variable edge size was defined for the solid mesh elements composing the free mesh pattern of each FE component, in order to preserve the computational cost of analyses. The size of elements was thus comprised within a minimum of 0.8mm (in the region of holes and bolts), up to 5mm (in the top region of the LG portion of the column). Such an assumption resulted in a total of 45,000 solid elements and 170,000 DOFs, for half geometry of the base connection mechanism.

The FE model was in fact further optimized, by accounting for symmetry conditions and by taking advantage of kinematic constraints (see Figure 5).

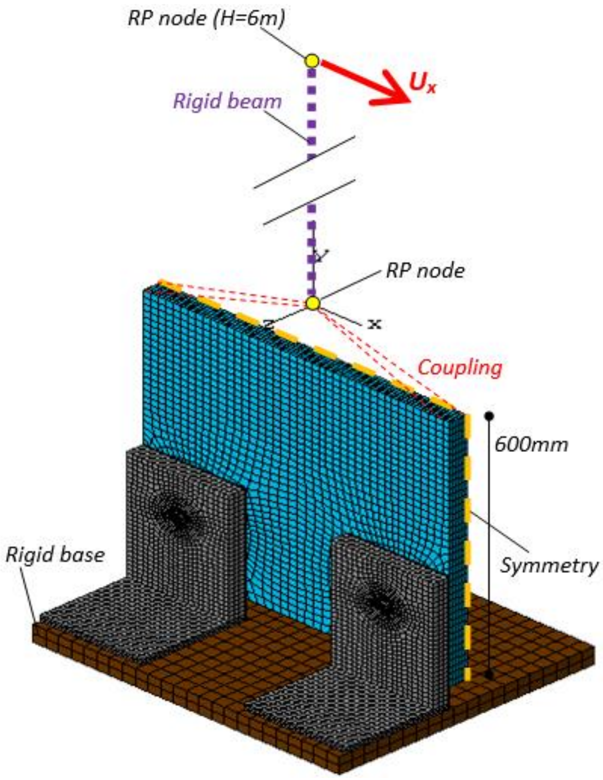

Figure 5. Refined FE numerical model of a base connection

A final attention was spent for the mechanical characterization of materials, in order to include possible damage initiation and propagation mechanisms in the seismic simulation (see (Santarsiero et al., 2019)). The intrinsic brittleness of glass, in particular, was accounted via the "Concrete Damaged Plasticity" (CDP) material model, and the key input features were derived from earlier research applications of the CDP approach to structural glass systems (further details can be found in (Santarsiero et al. 2018; Bedon & Louter, 2019). The nominal mechanical properties for the HS plates were taken into account, with E_g= 70GPa the MoE, ν_g= 0.23 the Poisson ratio and σ_{tk}= 70MPa the characteristic tensile resistance.

The characteristic compressive strength of glass was set equal to σ_{ck}= 1000MPa, for comparative purposes. Later, the stress evolution was continuously monitored during the simulation. It is in fact well known that the actual compression resistance may be in the order of 350-500MPa, and further dedicated studies / experiments should be necessarily carried out, in support of the FE outcomes reported in this paper.

5.2 *Results and comparisons*

From a practical point of view, accurate FE numerical investigations can represent a useful background for the detailing of restraints, as well as a robust tool with respect to simplified approaches (even geometrically refined) accounting for the angle brackets only.

However, some reliable calculations were found also from the analytical formulation of section 4, for the examined frame structure.

In terms of expected *q*-behaviour factor, in particular, comparative data are proposed in Table 6. There, the collected data are referred to three different modelling approaches, that is:

- the analytical estimates (i.e., section 4), and
- the numerical calculations from the FE model of Figure 5, and
- the numerical calculations from a FE model derived from Figure 5, but representative of a single angle bracket only (with equivalent boundaries).

Table 6. Comparative calculations of the expected ductility and theoretical behaviour factor of the case-study system. * ε_{max}= 15% and Δ= 10%

	Reference model		
	Analytical	3D “bracket”	3D “assembly”
δ_y [mm]	0.677	0.679	0.679
δ_u [mm]	63.98	54.10	39.39 *
μ	94.50	79.67	50.03 *
q	13.71	12.58	10.72 *

In Table 6, it is thus interesting to notice that the analytical model and the “bracket” FE model are able to offer a relatively good agreement, thus suggesting a certain potential of the analytical model of section 4. A good correlation ca be observed – at yielding – also for the 3D “assembly” FE model of Figure 5.

In terms of ultimate configuration of the glass frame – and thus corresponding q-factor estimates of Table 6 – some further considerations must be spent. Certainly, the overall seismic design process must account for additional key performance parameters, like for example the evolution of stress peaks in glass (especially in the region of holes – Figure 3), that the single bracket approach is not able to include. In this regard, the FE simulation of the full glazed assembly was stopped at a maximum top lateral drift of 10% (corresponding to 0.6m of lateral displacement for the frame). Such an ultimate condition was chosen based on the relatively high amplitude of lateral displacements, while it does not necessarily reflects any kind of damage in glass (or steel). In any case, the chosen failure configuration directly reflects on the calculated behaviour factor of Table 6, and justifies the relatively high scatter between the “bracket” estimates and the “assembly” results.

Another relevant aspect of Table 6 is that the *q*-estimates do not reflect the overall seismic performance of glass frames in general, but must be necessarily related to the geometrical and mechanical details in use.

As far as further relevant performance parameters are taken into account, in fact, both the potentials and limits of the analytical model of section 4 (as well as different FE modelling approaches) can be further emphasized. Moreover, more detailed estimated for the *q*-behaviour factor can be obtained.

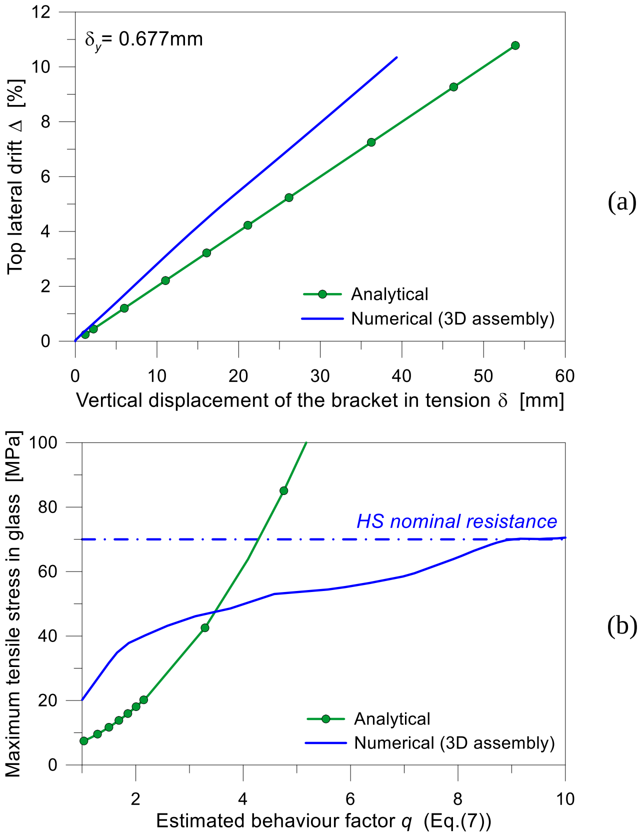

Figure 6. Analytical and numerical (ABAQUS) variation of (a) top lateral drift vs. vertical displacement of the bracket in tension and (b) stress peak near the glass hole in tension, as a function of the expected behaviour factor *q*

In Figure 6(a), for example, it is possible to notice that the evolution of the top lateral drift of the frame (Δ), represented as a function of the vertical deformation δ of the brackets in tension – as predicted by the “full system” FE model – is mostly linear but partly underestimated by the analytical model. Given that the behaviour of a single angle bracket is only taken into account by the analytical method, such an outcome certainly suggests the high potential and accuracy of the formulation.

When the stress evolution near the glass hole in tension is also considered (i.e., Figure 3), however, the "assembly" numerical model clearly gives evidence of the progressive plastification of the steel brackets, with a corresponding redistribution and non-linear evolution of stress peaks in glass (Figure 6(b)). There, the estimated behaviour factor q is also proposed, as derived – for each stress value – from the corresponding deformation of the bracket in tension. It can be thus seen that the higher is the expected stress peak (due to the imposed in-plane lateral deformations) and the higher is the expected dissipation capacity of the angle brackets in use, thus the maximum mitigation and enhanced performance of the whole frame can be exploited.

As far as the "assembly" FE estimates of Figure 6(b) are taken into account, for example, a potential q= 3-4 behaviour factor could be estimated for the examined glass frame, so as to preserve the glass members from severe stress concentrations.

In the same figure, however, it is also possible to see that the analytical expressions proposed in section 4 – and their combination with Eqs.(6)-(7) for the stress peaks estimates – can only roughly capture the actual non-linear behaviour of the examined 3D assembly, thus resulting in the comparative plots of Figure 6(b). Besides the intrinsic simplifications of the analytical formulations, however, could be used for preliminary calculations, in support of the definition of the key geometrical features of glazed frame systems.

6 SUMMARY AND CONCLUSIONS

The analytical and numerical results summarized in this paper for a case-study glass frame highlighted that the considered structural typology – when properly detailed against seismic events or other in-plane lateral loads – can exhibit enhanced ductility and offer a large amount of dissipative capacity, even in presence of a relatively tensile brittle, weak and vulnerable load-bearing material like glass.

More in detail, it was observed that even remarkable values of behaviour factor q can be theoretically expected for glass frames with push-pull base connections (i.e., Table 6).

Given the case-study example, the structural performance of the system proved to exhibit an higher dissipation capacity, compared to typical moment resisting frames composed of traditional load-bearing sections. It is in fact worth mentioning that the Eurocode suggests a behaviour factor in the range of q= 4-5.5 for moment resisting frame systems.

However, the estimates of Table 6 do not account for all the relevant performance parameters of interest for glas frames, and more in detail for the prevention of stress peaks in glass. From the above considerations, and based Figure 6(b), a conservative behaviour factor equal to q=2-3 (but in any case > 1) could be potentially assumed in practice, hence allowing for a reduction of the design seismic spectrum up to ≈70-80% the nominal value.

Certainly, it is also recognized that extended detailed studies should be still spent for the definition of a reliable behaviour factor calculation approach. Special care should be focused for various project configurations and joint details. Possibly, a robust extended experimental validation, inclusive of several geometrical and mechanical solutions of technical interest, should be carried out in support of a further refinement of major analytical and numerical outcomes.

REFERENCES

Bedon, C., Amadio, C., 2018. Numerical assessment of vibration control systems for multi-hazard design and mitigation of glass curtain walls. *Journal of Building Engineering*, **15**, 1-13

Bedon, C., Louter, C., 2019. Structural glass beams with embedded GFRP, CFRP or steel reinforcement rods; comparative experimental, analytical and numerical investigations. Journal of Building Engineering, 22: 227241

Bedon, C., Zhang, X., Santos, F., Honfi, D., Kozlowski, M., Arrigoni, M., Figuli, L., Lange, D., 2018. Performance of structural glass facades under extreme loads – Design methods, existing research, current issues and trends. *Construction and Building Materials*, **163**, 921-937

Casagrande, L., Bonati, A., Occhiuzzi, A., Caterino, N., Auricchio, F., 2019. Numerical investigation on the seismic dissipation of glazed curtain wall equipped on high-rise buildings. *Engineering Structures*, **179**, 225-245

CNR-DT 210/2013. Istruzioni per la progettazione, l'esecuzione ed il controllo di costruzioni con elementi strutturali di vetro. CNR, Roma (I), free download: www.cnr.it/it/node/2630

EN 1998-1:2004. Design of structures for earthquake resistance – Part 1: general rules, seismic actions and rules for buildings. CEN, Brussels, Belgium

Feldmann, M., Kasper, R., et al., 2014. Guidance for European Structural Design of Glass Components –

Support to the implementation, harmonization and further development of the Eurocodes. *Report EUR 26439 – Joint Research Centre – Institute for the Protection and Security of the Citizen*. (Eds.) Dimova, Pinto, Feldmann, Denton, doi: 10.2788/5523

Krstevska, L., Tashkov, L., Rajcic, V., Zarnic, R., 2013. Seismic behaviour of composite panel composed of laminated wood and bearing glass – experimental investigation. *Advanced Materials Research*, **778**, 698-705

Martins, L., Delgado, R., 2012. Seismic behavior of point supported glass panels. *Proceedings of Challenging Glass 3 – Conference on Architectural and Structural Applications of Glass*. (Eds.) Bos, Louter, Nijsse, Veer. TU Delft, June 2012

Mocibob, D., 2008. Glass panel under shear loading – Use of glass envelopes in building stabilization. PhD These n. 4185, EPFL Lausanne, Lausanne, Switzerland. Available online: https://infoscience.epfl.ch/record/125889/files/

NTC2018. Norme Tecniche per le Costruzioni, Ministero delle Infrastrutture e dei Trasporti, Decreto Ministeriale 17 gennaio 2018

Santarsiero, M., Bedon, C., Moupagitsoglou, K., 2019. Energy-based considerations for the seismic design of ductile and dissipative glass frames. *Soil Dynamics and Earthquake Engineering*, **125**, 105170

Santarsiero, M., Bedon, C., Louter, C., 2018. Experimental and numerical analysis of thick embedded laminated glass connections. Composite Structures, 188: 242-256

Simulia (2019). ABAQUS computer software

Sivanerupan, S., Wilson, J.L., Gad, E.F., 2011. Structural analysis and design of glazed curtain wall systems. *Australian Journal of Structural Engineering*, **12**, 57-67

Sivanerupan, S., Wilson, J.L., Gad, E.F., Lam, N.T.K., 2014. Drift performance of point fixed glass façade systems. *Advances in Structural Engineering*, **17**(10), 1481-1495

Sucuoglu, H., Vallabhan, C.V.G., 1997. Behaviour of window glass panels during earthquakes. *Engineering Structures*, **19**(8), 685-694

Wensheng, L., Baofeng, H., 2008. Discussion on seismic performance indexes of architectural curtain walls. *Proceedings of the 14th WCEE Conference – World Conference on Earthquake Engineering*, October 12-17, 2008, Beijing, China